

Growth and thermal conductivity analysis of polycrystalline GaAs on chemical vapor deposition diamond for use in thermal management of high-power semiconductor lasers

S. P. R. Clark, P. Ahirwar, F. T. Jaeckel, C. P. Hains, A. R. Albrecht et al.

Citation: *J. Vac. Sci. Technol. B* **29**, 03C130 (2011); doi: 10.1116/1.3565054

View online: <http://dx.doi.org/10.1116/1.3565054>

View Table of Contents: <http://avspublications.org/resource/1/JVTBD9/v29/i3>

Published by the AVS: Science & Technology of Materials, Interfaces, and Processing

Related Articles

Epitaxial strontium titanate films grown by atomic layer deposition on SrTiO₃-buffered Si(001) substrates
J. Vac. Sci. Technol. A **31**, 01A136 (2013)

Comparison of beryllium oxide and pyrolytic graphite crucibles for boron doped silicon epitaxy
J. Vac. Sci. Technol. A **30**, 061603 (2012)

Template-dependent nucleation of metallic droplets
J. Vac. Sci. Technol. B **30**, 060603 (2012)

Formation and morphological evolution of InAs quantum dots grown by chemical beam epitaxy
J. Vac. Sci. Technol. B **30**, 051207 (2012)

Growth of epitaxial oxides on silicon using atomic layer deposition: Crystallization and annealing of TiO₂ on SrTiO₃-buffered Si(001)
J. Vac. Sci. Technol. B **30**, 04E111 (2012)

Additional information on *J. Vac. Sci. Technol. B*

Journal Homepage: <http://avspublications.org/jvstb>

Journal Information: http://avspublications.org/jvstb/about/about_the_journal

Top downloads: http://avspublications.org/jvstb/top_20_most_downloaded

Information for Authors: http://avspublications.org/jvstb/authors/information_for_contributors

ADVERTISEMENT

Instruments for advanced science

Gas Analysis



- dynamic measurement of reaction gas streams
- catalysis and thermal analysis
- molecular beam studies
- dissolved species probes
- fermentation, environmental and ecological studies

Surface Science



- UHV TPD
- SIMS
- end point detection in ion beam etch
- elemental imaging - surface mapping

Plasma Diagnostics



- plasma source characterization
- etch and deposition process reaction kinetic studies
- analysis of neutral and radical species

Vacuum Analysis



- partial pressure measurement and control of process gases
- reactive sputter process control
- vacuum diagnostics
- vacuum coating process monitoring

contact Hiden Analytical for further details

HIDEN ANALYTICAL

info@hideninc.com
www.HidenAnalytical.com
CLICK to view our product catalogue

Growth and thermal conductivity analysis of polycrystalline GaAs on chemical vapor deposition diamond for use in thermal management of high-power semiconductor lasers

S. P. R. Clark,^{a)} P. Ahirwar, F. T. Jaeckel, C. P. Hains, A. R. Albrecht, T. J. Rotter, L. R. Dawson, and G. Balakrishnan
Center for High Technology Materials, University of New Mexico, 1313 Goddard SE, Albuquerque, New Mexico 87106

P. E. Hopkins and L. M. Phinney
Sandia National Laboratories, P.O. Box 5800, Albuquerque, New Mexico 87185

J. Hader and J. V. Moloney
College of Optical Sciences, University of Arizona, Tucson, Arizona 85721

(Received 27 October 2010; accepted 20 February 2011; published 11 April 2011)

The authors demonstrate the growth of polycrystalline GaAs thin films on polycrystalline chemical vapor deposition (CVD) diamond by low-temperature molecular beam epitaxy. The low-temperature GaAs (LT-GaAs) layer is easily polished compared to the CVD diamond, and this process results in a reduction of rms surface roughness from >50 to <5 nm. This makes the LT-GaAs on diamond layer an ideal wafer-bonding interface for high-power semiconductor devices. The samples were grown at $0.2 \mu\text{m/h}$ with a substrate temperature of 250°C and a 1:8 III/V beam equivalent pressure ratio. The samples were analyzed by x-ray powder diffraction, atomic force microscopy for surface roughness, and *in situ* reflective high-energy electron diffraction during molecular beam epitaxy growth. The authors also measure the thermal conductivity of the GaAs layer on CVD diamond using pump-probe time domain thermoreflectance.

© 2011 American Vacuum Society. [DOI: 10.1116/1.3565054]

I. INTRODUCTION

High-power semiconductor lasers, both electrically and optically pumped, are significantly limited in performance by the ability to extract heat from the active region. In the case of optically pumped lasers such as vertical external cavity surface emitting lasers (VECSELs), a semiconductor chip is pumped with as much as 150 W continuous wave (CW) over a $500 \mu\text{m}$ diameter pump spot.¹ This optical pumping results in power densities in excess of 19 kW/cm^2 and translates to an active region temperature of over 375 K .¹ Any further increase in active region temperature can result in significantly reduced gain, which induces thermal rollover of the laser. In the absence of any thermal management, heat in the active region allows the laser to operate at only a few watts before thermal rollover.¹⁻³ Thermal management strategies started with the use of copper heat sinks and thermoelectric coolers and the advent of high-power lasers has evolved to include heat spreaders. Heat spreaders such as diamond sit between the heat source and the heat sink and have the ability to spread a localized thermal accumulation over a large area very quickly.^{2,3} Thus, heat spreaders allow the underlying sink to remove the heat more efficiently from the active region.

Single-crystal diamond is one of the most effective heat spreaders due to a thermal conductivity of $\sim 2000 \text{ W m}^{-1} \text{ K}^{-1}$,^{4,5} which is the highest of any known naturally occurring material. In the context of high-power

VECSELs, single crystal diamond has been used as both external heat spreaders and as intracavity heat spreaders.² The primary mechanism for bonding the semiconductor laser to diamond is by soldering or capillary bonding. In case of a solder bond, the interfacial quality is not too critical. However, for a capillary bond to form, the two surfaces have to be flat on an atomic scale. This interface quality is very high in case of a single crystal diamond and can be bonded effectively to semiconductor surfaces. The major drawback with the use of single crystal diamond is the low availability and high cost of the material. Recently, chemical vapor deposition (CVD) diamond has emerged as a relatively cheap alternative, with similar thermal conductivity values ($>1800 \text{ W m}^{-1} \text{ K}^{-1}$) to single crystal diamond.⁴ However, despite polishing, CVD diamond is too rough to be capillary bonded or wafer bonded to the semiconductor laser and hence its integration with the semiconductor is limited to soldering. The use of solder, in this case, indium, significantly limits the rate at which the heat can be extracted from the active region into the diamond.^{4,5} Thus, the indium solder layers, which are $10\text{--}50 \mu\text{m}$ in thickness, act as thermal bottlenecks. Furthermore, the indium tends to form voids at the soldering interface and can lead to very high local thermal resistance thus damaging the chip during operation.⁵ Despite these limitations, semiconductor/CVD-diamond soldering has resulted in some of the highest-power VECSELs to date with an output power of $\sim 50 \text{ W CW}$ at 1040 nm .⁶ Theoretical studies have indicated that much higher output power levels can be achieved from these lasers. The clamp-

^{a)}Electronic mail: sprclark@chtm.unm.edu

ing of the output power at ~ 50 W is primarily due to thermal bottlenecks at the semiconductor/diamond and the diamond/copper interfaces.^{1,2,4}

A different approach to the integration of CVD diamond with semiconductors can be achieved by the growth of a thin polycrystalline film of the semiconductor on the CVD-diamond substrate. The semiconductor is subsequently polished to a surface roughness of approximately $\sim 1\text{--}5$ nm which makes it suitable as a wafer-bonding interface. The process of wafer-bonding III-V single crystals to polycrystalline or amorphous thin films is well described elsewhere.⁷ This approach completely eliminates the need for any indium solder between the semiconductor and the CVD diamond. The absence of indium allows the active region to be brought extremely close ($1\text{--}5$ μm) to the diamond heat spreader. The semiconductor grown on the diamond is able to bond more effectively to the rough diamond surface and completely eliminates the issue of voids at the interface.

In this paper, we discuss the growth, characterization, and thermal properties of polycrystalline GaAs thin films grown on CVD diamond with an ultimate objective of using such films as wafer-bonding interfaces. The semiconductor buffer layers are grown using low-temperature molecular beam epitaxy (LT-MBE) on Element 6[®] TM180[®] thermal management grade CVD-diamond wafers which have thermal conductivities of >1800 $\text{W m}^{-1} \text{K}^{-1}$. The GaAs on diamond layers are then polished to achieve as smooth a surface as possible for wafer bonding. The films are characterized using atomic force microscopy (AFM) and powder x-ray diffraction (XRD). Finally, we measure the thermal conductance of the grown thin films using pump-probe time domain thermoreflectance (TDTR) and we compare its performance to indium based solders.

II. EXPERIMENT

The structures were grown using a VG V80H elemental source molecular beam epitaxy reactor. The residual surface contaminants on the diamond substrates were thermally removed by heating the sample at 400 $^{\circ}\text{C}$ for ~ 30 min in a preparation chamber in the MBE reactor. The substrate was then transferred into the growth chamber where LT-GaAs was grown using well-established growth parameters⁸ of 250 $^{\circ}\text{C}$ substrate temperature, 0.2 $\mu\text{m/h}$ GaAs single crystal growth rate, and a III/V beam equivalent pressure ratio of 1:8. The substrate temperature was controlled by a substrate heater thermocouple since our pyrometry setup is only capable of measuring above 440 $^{\circ}\text{C}$. A set of samples was grown with the GaAs film thickness varying from 100 nm to 5 μm .

III. RESULTS AND DISCUSSION

Figures 1(a) and 1(b) show reflection high-energy electron diffraction (RHEED) patterns of CVD diamond and polycrystalline GaAs during growth. The electron gun for this experiment is set at 12.4 kV and filament current is set to 1.4 A. The RHEED pattern for CVD diamond consists of irregular spots indicating a highly polycrystalline substrate. The

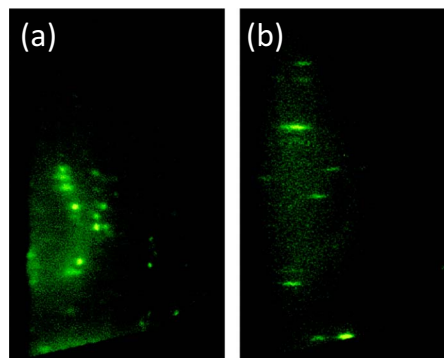


FIG. 1. (Color online) Reflective high-energy electron diffraction pattern of (a) CVD-diamond substrate and (b) GaAs on CVD diamond. The RHEED pattern shows a highly polycrystalline CVD-diamond substrate and the GaAs layer also shows a similar polycrystalline signature with more streaks indicating reduced roughness.

RHEED pattern from the GaAs films on diamond proceeds in a very similar manner to polycrystalline GaAs that has been observed on other substrates.^{8,9} The growth progresses with the spots evolving into streaks indicating a smoother GaAs surface. The GaAs film, however, remains polycrystalline. Furthermore, the streaked RHEED pattern from the GaAs does not appear on all areas of the sample. There is a total absence of such patterns in some areas when the electron beam spot is moved around on the sample. This indicates that the growth is a mixture of amorphous and polycrystalline GaAs. In the thicker samples there are larger areas over which a RHEED pattern can be seen indicating improved polycrystalline material.

Figure 2(a) shows the topography, measured by AFM, of a CVD-diamond substrate. The CVD-diamond substrate's rms surface roughness varies typically between 50 and 100 nm. As mentioned in the introductory paragraphs, this is the CVD-diamond surface to which researchers have bonded a variety of devices to spread heat.¹⁻³ The growth of LT-GaAs layers on CVD diamond leads to a significant reduction in surface roughness. Figure 2(b) shows an AFM surface scan of LT-GaAs on diamond, which has a rms surface roughness of $10\text{--}15$ nm. Finally, this surface can be further smoothed by polishing, which reduces the surface roughness to $3\text{--}5$ nm (rms) as shown in Fig. 2(c). The samples were polished with a soft polishing pad and colloidal silica polishing suspension. The average particle size for colloidal silica polishing suspensions ranges between 0.04 and 0.07 μm . The LT-GaAs films adhere very well to the diamond and we do not observe any chipping or flaking of the GaAs film. Further reductions in the GaAs surface roughness can be achieved using chemical mechanical polishing.

The polycrystalline nature of the GaAs film was confirmed by powder x-ray diffraction. Figure 3 shows an omega-2 theta scan of a $5\text{-}\mu\text{m}$ -thick GaAs layer grown on CVD diamond. The diffraction pattern was recorded using nonmonochromatic $\text{Cu K}\alpha$ radiation on a Panalytical powder diffractometer and the $\text{Cu K}\alpha 2$ contribution was subtracted for clarity.¹⁰ Besides the diamond (111) reflection, the GaAs (111), (220), and (311) reflections are clearly developed. We

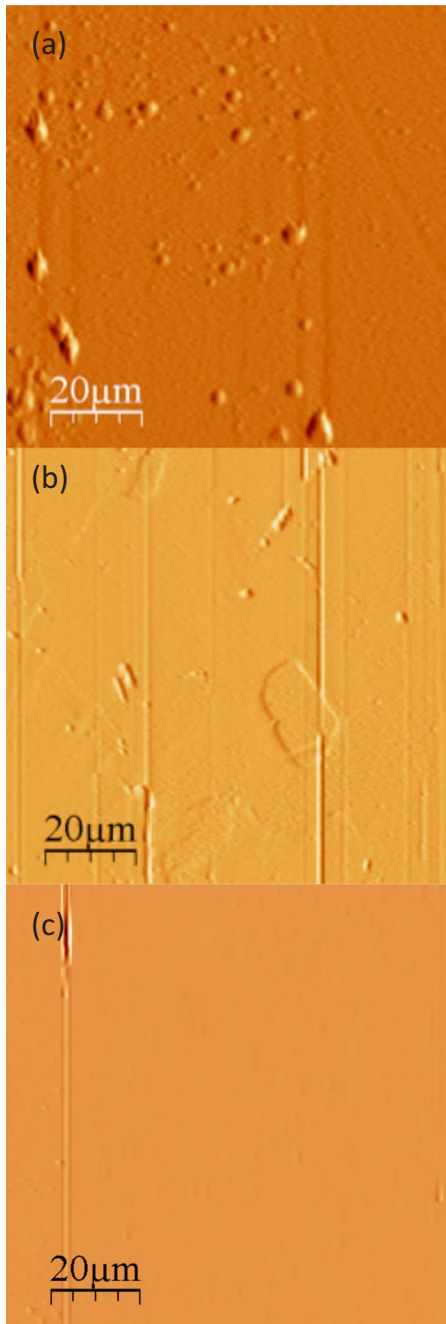


FIG. 2. (Color online) AFM surface scans of (a) CVD diamond, (b) poly-GaAs on CVD diamond, and (c) polished poly-GaAs on CVD diamond. The surface roughness reduces significantly in the three cases: from >50 nm rms for the diamond, to 10–15 nm for the poly-GaAs on the diamond, to finally 1–5 nm rms for the polished poly-GaAs on diamond.

do not find any evidence for other phases. While pole figures have not been recorded, the relative peak intensities of the GaAs reflections lead us to speculate that there is very little preferred orientation. We cannot exclude the presence of significant amounts of amorphous GaAs in our films on the basis of this scan. It is extremely difficult to conduct cross-section transmission electron microscopy on these samples in order to further characterize the polycrystalline GaAs grain size since the cleaving and ion milling of the samples on diamond is a nontrivial issue.

JVST B - Microelectronics and Nanometer Structures

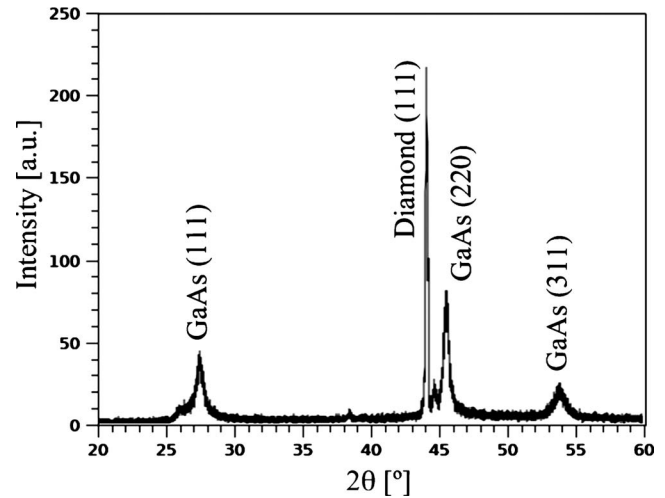


FIG. 3. Omega-2 theta XRD scan of a 5- μm -thick GaAs growth on CVD diamond. The diamond (111) plane and the GaAs (111), (220), and (311) planes are clearly developed.

Finally, we measured the thermal conductivity of the polycrystalline GaAs films with a pump-probe TDTR setup located at the Sandia National Laboratories. Details of the experimental setup and thermal analysis are discussed in detail elsewhere.^{11,12} We coat the polycrystalline GaAs films with a 100 nm Al transducer layer. We modulate the pump-heating event at 11 MHz to make the effects of radial transport negligible ensuring that we accurately resolve the cross plane thermal conductivity of the thin polycrystalline GaAs film. For the thermal analysis, we measure the electrical resistivity of the Al transducer with a four point probe and determine the thermal conductivity to be $200 \text{ W m}^{-1} \text{ K}^{-1}$. We assume published values for the thermal conductivity and heat capacity of bulk diamond substrate and the heat capacity of the GaAs film ($1.74 \text{ MJ m}^{-3} \text{ K}^{-1}$).¹³ From the best fit of the thermal model to the data, as shown in Fig. 4, the thermal conductivities of the 1- μm -, 500-nm-, and 100-nm-thick polycrystalline GaAs films are 14.5, 10.4, and $8.1 \text{ W m}^{-1} \text{ K}^{-1}$, respectively. These values are reduced from

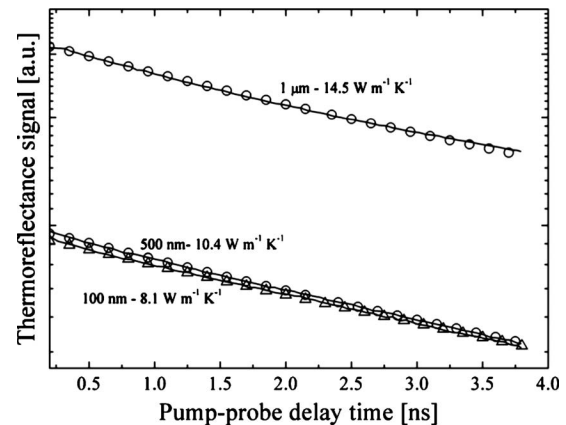


FIG. 4. Thermal conductivities of 1 μm , 500 nm, and 100 nm poly-GaAs films on CVD diamond as measured using pump-probe time domain thermoreflectance.

the thermal conductivity from single crystal bulk GaAs ($46 \text{ W m}^{-1} \text{ K}^{-1}$).¹² This reduction is expected due to the polycrystalline nature of the GaAs films which will increase phonon scattering events.^{14,15} In addition, the decrease in value with decrease in film thickness is expected due to increased size effects, creating additional phonon scattering events, as the film becomes thinner. Also extracted from the measurements are the thermal boundary conductances at the Al/polycrystalline GaAs (on all samples) and polycrystalline GaAs/diamond interfaces (on the 100 nm polycrystalline GaAs sample), which are determined as 30 and $40 \text{ MW m}^{-2} \text{ K}^{-1}$, respectively. The Al/polycrystalline GaAs thermal boundary conductance is low compared to typical values for metal/single crystal dielectric interfaces,¹⁶ but the polycrystalline nature of the GaAs film could induce disorder around the interface causing a decrease in the thermal boundary conductance.¹⁷⁻²⁰

From the thermal measurements, the polycrystalline GaAs films show promise as an improved thermal interface material (TIM) for diamond heat sinks over traditionally used indium solders. Typical indium solder thermal interface materials have thicknesses on the order of several microns. Assuming a bulk value for the thermal conductivity of In ($81.8 \text{ W m}^{-1} \text{ K}^{-1}$), the thermal resistance of a $10 \text{ }\mu\text{m}$ TIM of In is $1.22 \times 10^{-7} \text{ m}^2 \text{ K W}^{-1}$. Although the thermal conductivities of the polycrystalline GaAs films are less than that of bulk indium, the required film thickness is much lower than the typical thickness of In used as TIMs. For the 100 nm polycrystalline GaAs films measured in this study, the thermal resistance is $1.2 \times 10^{-8} \text{ m}^2 \text{ K W}^{-1}$, a thermal resistance that is a factor of 10 lower than a traditional In TIM.

IV. SUMMARY AND CONCLUSIONS

In conclusion, polycrystalline GaAs layers have been grown on CVD-diamond using LT-MBE. The polycrystalline nature of the films is verified using RHEED and x-ray diffraction experiments. The LT-GaAs layer is polished resulting in a final surface roughness that is $<5 \text{ nm rms}$. The samples are grown at $0.2 \text{ }\mu\text{m/h}$ with a substrate temperature of $250 \text{ }^\circ\text{C}$ and a 1:8 III/V beam flux ratio. The GaAs films are further characterized for thermal conductivity using TDTR techniques and results in thermal conductivity values of 14.5, 10.4, and $8.1 \text{ W m}^{-1} \text{ K}^{-1}$, respectively, for the 1 μm , 500 nm, and 100 nm polycrystalline GaAs films.

ACKNOWLEDGMENTS

This research is done at the University of New Mexico and the University of Arizona for this publication and was funded by a U.S. Joint Technology Office Multidisciplinary Research Initiative Program, AFOSR Grant No. FA9550-07-1-0573 and Optoelectronics Research Center (at CHTM), AFOSR Grant No. FA9550-09-1-0202. P.E.H is grateful for funding from the LDRD program office through the Sandia National Laboratories Harry S. Truman Fellowship. Sandia is a multiprogram laboratory operated by Sandia Corporation, a Lockheed-Martin Company, for the United States Department of Energy's National Nuclear Security Administration under Contract No. DE-AC04-94AL85000.

- ¹A. R. Zakharian, J. Hader, J. V. Moloney, S. W. Koch, P. Brick, and S. Lutgen, *Appl. Phys. Lett.* **83**, 1313 (2003).
- ²K. S. Kim, J. R. Yoo, S. H. Cho, S. M. Lee, S. J. Lim, J. Y. Kim, J. H. Lee, T. Kim, and Y. J. Park, *Appl. Phys. Lett.* **88**, 091107 (2006).
- ³B. Rösener, N. Schulz, M. Rattunde, C. Manz, K. Köhler, and J. Wagner, *Proc. SPIE* **6997**, 699702 (2008).
- ⁴S. S. Dahlgren and H. T. Hall, Jr., *Thermal and Thermomechanical Phenomena in Electronic Systems*, IThERM, 2000 Vol. 1, p. 303.
- ⁵X. Liu, R. W. Davis, L. C. Hughes, M. H. Rasmussen, R. Bhat, and C.-E. Zah, *J. Appl. Phys.* **100**, 013104 (2006).
- ⁶Y.-Y. Lai, J. M. Yarborough, Y. Kaneda, J. Hader, J. V. Moloney, T. J. Rotter, G. Balakrishnan, C. Hains, and S. W. Koch, *IEEE Photonics Technol. Lett.*, **22**, 1253 (2010).
- ⁷F. F. Shi, K.-L. Chang, and K. C. Hsieh, *J. Phys. D* **40**, 7694 (2007).
- ⁸A. Shen, H. Ohno, Y. Horikoshi, S. P. Guo, Y. Ohno, and F. Matsukura, *Appl. Surf. Sci.* **130-132**, 382 (1998).
- ⁹M. Mosaddequr Rahman, T. Soga, and T. Jimbo, *Advanced Nanomaterials and Nanodevices* (IUMRS-ICEM, Xi'an, 2002).
- ¹⁰C. Dong, H. Chen, and F. Wu, *J. Appl. Crystallogr.* **32**, 168 (1999).
- ¹¹P. E. Hopkins, J. R. Serrano, L. M. Phinney, S. P. Kearney, T. W. Grasser, and C. T. Harris, *J. Heat Transfer* **132**, 081302 (2010).
- ¹²D. G. Cahill, *Rev. Sci. Instrum.* **75**, 5119 (2004).
- ¹³S. M. Sze, *Physics of Semiconductor Devices*, 2nd ed. (Wiley, New York, 1981).
- ¹⁴A. D. McConnell and K. E. Goodson, *Annu. Rev. Heat Transfer* **14**, 129 (2005).
- ¹⁵A. D. McConnell, S. Uma, and K. E. Goodson, *J. Microelectromech. Syst.* **10**, 360 (2001).
- ¹⁶R. J. Stevens, A. N. Smith, and P. M. Norris, *J. Heat Transfer* **127**, 315 (2005).
- ¹⁷T. E. Beechem, S. Graham, P. E. Hopkins, and P. M. Norris, *Appl. Phys. Lett.* **90**, 054104 (2007).
- ¹⁸P. E. Hopkins, L. M. Phinney, J. R. Serrano, and T. E. Beechem, *Phys. Rev. B* **82**, 085307 (2010).
- ¹⁹P. E. Hopkins, P. M. Norris, R. J. Stevens, T. Beechem, and S. Graham, *J. Heat Transfer* **130**, 062402 (2008).
- ²⁰T. Beechem and P. E. Hopkins, *J. Appl. Phys.* **106**, 124301 (2009).